Behavioral/Systems/Cognitive

Neural Activity Associated with the Passive Prediction of Ambiguity and Risk for Aversive Events

Dominik R. Bach, Ben Seymour, and Raymond J. Dolan
Wellcome Trust Centre for Neuroimaging, University College London, London WC1N 3BG, United Kingdom

In economic decision making, outcomes are described in terms of risk (uncertain outcomes with certain probabilities) and ambiguity (uncertain outcomes with uncertain probabilities). Humans are more averse to ambiguity than to risk, with a distinct neural system suggested as mediating this effect. However, there has been no clear disambiguation of activity related to decisions themselves from perceptual processing of ambiguity. In a functional magnetic resonance imaging (fMRI) experiment, we contrasted ambiguity, defined as a lack of information about outcome probabilities, to risk, where outcome probabilities are known, or ignorance, where outcomes are completely unknown and unknowable. We modified previously learned pavlovian CS+ stimuli such that they became an ambiguous cue and contrasted evoked brain activity both with an unmodified predictive CS+ (risky cue), and a cue that conveyed no information about outcome probabilities (ignorance cue). Compared with risk, ambiguous cues elicited activity in posterior inferior frontal gyrus and posterior parietal cortex during outcome anticipation. Furthermore, a similar set of regions was activated when ambiguous cues were compared with ignorance cues. Thus, regions previously shown to be engaged by decisions about ambiguous rewarding outcomes are also engaged by ambiguous outcome prediction in the context of aversive outcomes. Moreover, activation in these regions was seen even when no actual decision is made. Our findings suggest that these regions subserve a general function of contextual analysis when search for hidden information during outcome anticipation is both necessary and meaningful.

Key words: **ambiguity; risk; uncertainty; probability distribution; probabilistic outcome prediction; pavlovian conditioning; fear conditioning; fMRI; BOLD**

Introduction

Many predictions an organism makes about the world contain uncertainty. In decision making, economists distinguish different kinds of uncertainty. Risk refers to situations in which we know the precise probabilities of each outcome (Bernoulli, 1738). Decision making under risk is axiomized in expected utility theory to provide the basis of rational choice (von Neumann and Morgenstern, 1944). These axioms are violated when outcome probabilities are not known with certainty (that is, they do not correspond to a point estimate), a situation referred to as ambiguity (Ellsberg, 1961).

People tend to avoid outcomes associated with ambiguity (Becker and Brownson, 1964; Slovic and Tversky, 1974; Larson, 1980; Curley et al., 1986; Pulford and Colman, 2008), where one critical feature is lack of information about outcome probabilities (Larson, 1980; Camerer, 1995). It has been suggested that the amygdala and dorsomedial prefrontal and orbitofrontal cortex mediate decision making under ambiguity (Hsu et al., 2005). However, choices based on ambiguous monetary gambles are also reported to engage lateral prefrontal cortex, anterior insula, and parietal regions (Huettel et al., 2006). A limitation of both these studies is that they conflate activity associated with the perception of ambiguity and decisions that ensue from this perception. Brain activations in these studies might therefore be attributable to decision making as well as to what has been termed in a recent neuroeconomic framework the representation process, that is, the identification and assessment of external and internal states (Rangel et al., 2008). Furthermore, since both studies used ambiguous rewarding outcomes, it is not known whether brain areas activated in these studies also encode ambiguity about aversive outcomes.

The importance of a distinction between outcome prediction with, and without, choice is embedded in theoretical accounts of a distinction between pavlovian and instrumental conditioning. Thus, pavlovian conditioning has often been used to study the distinction between prediction and control (Dayan and Balleine, 2002). Accordingly, to study the neural basis of ambiguity perception per se, we used a pavlovian conditioning procedure and provided participants with ambiguous situations in which an outcome prediction is made, but no actual decision required. Within this context, we defined ambiguity as "*known-to-be-missing information*, or not knowing relevant information that could be known" (Camerer, 1995; p. 645). This definition of ambiguity implies the fact that information is hidden from the observer, and draws distinction with ignorance, in which probabilities of outcomes are unknown, but are also unknowable (unless exploration and learning are permitted).

Received Sept. 23, 2008; revised Nov. 4, 2008; accepted Dec. 22, 2008.

This work was supported by a Programme grant to R.J.D. from the Wellcome Trust and by a Personal grant to D.R.B. from the Swiss National Science Foundation. We thank Mkael Symmonds for many helpful discussions.

This article is freely available online through the *J Neurosci* Open Choice option.

Correspondence should be addressed to Dominik R. Bach, Wellcome Trust Centre for Neuroimaging, 12 Queen Square, London WC1N 3BG, UK. E-mail: d.bach@fil.ion.ucl.ac.uk.

DOI:10.1523/JNEUROSCI.4578-08.2009

 0270-6474/09/291648-09$15.00/0

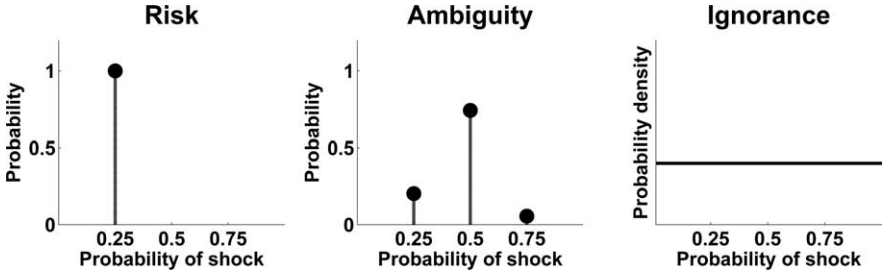

Figure 1. Examples for outcome prediction after risky, ambiguous, or ignorance cues, visualized by a second-order distribution of outcome probabilities. In the risk condition, prediction of outcome probability corresponds to a point estimate (left). In ambiguous trials, outcome probabilities can be predicted using a second-order distribution, thus rendering outcome predictions probabilistic. Ignorance cues convey no information about outcomes, the outcome probability could therefore have any value, and its prediction corresponds to a uniform distribution.

We degraded previously learned conditioned visual stimuli (CS+) so that, under the ambiguity condition, they only allowed a probabilistic prediction of outcome probabilities. These stimuli were contrasted with the original CS+ that conveyed a point estimate of outcome probabilities. Critically, to distinguish responses to lack of information alone from lack of information that could potentially be known (that is, hidden information), we also included completely novel stimuli that carried no predictive information, thereby corresponding to a uniform prediction of outcome probabilities (Fig. 1). Thus, we could identify brain areas responding to probabilistic prediction of outcome probabilities as opposed to certain outcome probabilities and to completely unknown outcome probabilities. Our design ensured that on average, all conditions carried the same outcome probability.

Materials and Methods

Design and participants

The study used a pavlovian conditioning paradigm within a single factorial design with four levels (CS−, risk, ambiguity, and ignorance). Twenty healthy right-handed participants (10 male, 10 female, mean age ± SD: 27.4 ± 5.8 years) were recruited from the general population and given monetary compensation of £40 for participation. Handedness was controlled with the Edinburgh Handedness Inventory (Oldfield, 1971) (mean ± SD: 83.6 ± 23.2). All participants gave written informed consent, and the study was approved by the local ethics committee.

Independent variable

There were four levels for the independent variable "condition," which varied on each trial in an event-related design. (1) A perceptually distinct CS− served as internal baseline condition and signaled the absence of the UCS on this trial. (2) In the risk condition, one of three previously learned compound CS+'s, signaling three different CS–UCS contingencies, was presented with a white frame indicating that no additional noise was added. CS–UCS contingencies were 0.25, 0.50, and 0.75 respectively. (3) In the ambiguity condition, noise was added to the previously learned compound CS+ by randomly flipping its four information bits at a noise rate of 20% per bit. Thus, participants were unable to generate a point estimate of outcome probabilities, although a probabilistic prediction was possible by taking into account the second-order distribution of underlying risky CS+. This condition was signaled to participants by a gray frame around the CS+. Each of 16 possible stimuli appeared at least once, while their frequencies were determined by the noise rate. After the expectancy period, together with the UCS, the original underlying CS+ was shown on the screen. UCS contingency of ambiguous cues was determined by the UCS contingency of the underlying risky cue. Critically, occurrence of the underlying CS+, and thus the frequency of electric shocks, was identical between the risk and the ambiguity condition (Fig. 2*F*). (4) In the ignorance condition, a completely new set of CS+ was presented, which had the same internal structure and CS–UCS contingency as the ambiguity stimuli. However, different symbols were used, and the internal pattern of each stimulus was reversed from left to right. Thus, it was not possible to predict the outcome of these stimuli, and each single stimulus did not occur often enough to fully learn outcome contingencies.

Stimuli

CS. CS+ stimuli in all conditions consisted of four pieces (i.e., information bits) that could take two different states. In one stimulus set, a combination of four rectangles was used that could be either yellow or blue. In the other set, each of four geometrical symbols could be either a circle or a triangle (Fig. 2*B*). The use of these two stimulus sets was balanced across participants, so that one half received the colored rectangles as risk/ambiguity stimuli and the dark green symbols as ignorance stimuli, and vice versa for the other half. A white frame indicated the risk, or noiseless, condition, and a gray frame (40%) the ambiguity, or noise, condition (Fig. 2*C*,*D*). No frame was presented in the ignorance condition (Fig. 2*E*). A light blue rectangle without frame served as CS− in both stimulus sets (Fig. 2*A*). All stimuli were presented on a black background, randomly either above or below the screen center.

UCS. As unconditioned stimulus, participants received an aversive 500 Hz train of electrical pulses (square wave, individual pulse duration: 200 μs, total duration: 500 ms, individually adjusted current, mean ± SD: 14.3 ± 4.3 mA), delivered via pediatric ECG electrodes (DENIL10026, Spes Medica) to the left hand. Stimulation intensity was determined before the experiment started and was set slightly below the pain tolerance. After the procedure was explained to participants, discomfort and pain thresholds were roughly assessed with ascending stimulation intensity. Random stimulus intensities were then delivered around the pain threshold to establish a stimulus-percept function. The random procedure was repeated after the experiment. There was no change in perception of the stimuli between the preexperiment and postexperiment measurements ($p > 0.70$).

Experimental procedure

Pavlovian fear conditioning. After participants arrived in the laboratory, the task was fully explained and the UCS level was determined as described above. Participants then engaged in a pavlovian learning task to condition the different CS–UCS contingencies (CS−: no UCS, CS+: 0.25, 0.50, and 0.75). They were not informed about the nature of the learning task; however, instructions included a statement that "after some symbols, electric stimulation will be more frequent than after others." Pavlovian conditioning was conducted in the scanner environment with the scanner running to ensure an identical context between learning and the subsequent critical experimental paradigm. Each of the four CS (CS− and three CS+) occurred 20 times in pseudorandomized order.

To ensure learning, skin conductance responses (SCRs) were recorded in a subsample of 14 participants, while in the remaining 6 participants, SCR was not recorded due to a technical failure. Recordings were made on thenar/hypothenar of the left hand using 8 mm Ag/AgCl cup electrodes (EL258, Biopac Systems). Constant voltage was provided by an integrated skin conductance preamplifier (AT64, Autogenic Systems). The signal was converted to an optical pulse (minimum resolution 7 Hz), digitally converted with 100 Hz sampling rate (Micro1401, Cambridge Electronic Design), and recorded (Spike2, Cambridge Electronic Design). Further analysis was performed in Matlab (Version 7.1., MathWorks). The signal was temporally filtered with a bidirectional Gaussian kernel of 0.5 s full duration at half maximum and high-pass filtered with a first order Butterworth filter and a cutoff frequency of 0.0159 Hz, corresponding to a time constant of 10 s. After visual inspection for artifacts, anticipatory conditioned reaction was calculated as mean SCR during CS presentation, corrected for 1 s baseline before stimulus onset. Learning was modeled using a simple Rescorla–Wagner rule (Rescorla and Wagner, 1972), assuming a learning rate of $\alpha = 0.3$ and initial outcome prediction values of 0.5 for all four CS. For each individual participant, a trial-by-trial general linear model was then fitted, using

predicted outcome, variance of the outcome distribution, and prediction error on the last trial as regressors. Beta estimates of these models were analyzed on the group level using one-sample *t* tests. Responses to CS+ and CS− were additionally averaged across trials and analyzed in a one way ANOVA model using the GLM approach in SPM 12.0 (SPSS).

Scanning. After the pavlovian conditioning, the concept of noisy reception was explained as well as the occurrence of completely new symbols in the ignorance condition (see instructions in supplemental methods). During the scanning experiment, 45 stimuli for the risk, ambiguity, and ignorance conditions were presented in pseudorandomized order. Fifteen interspersed CS− served as internal baseline (that is, as null events) to allow recovery of blood oxygen level-dependent (BOLD) signal in regions of interest.

Intratrial procedure

At the beginning of each trial, a CS was presented for 5.2 s (Fig. 3). Participants were tasked to indicate the position of the CS (above or below the screen center) with a button press as quickly as possible, while between responses, they held down a resting button. After the CS disappeared, the outcome was signaled at the center of the screen by a lightning-style sign to indicate shock (which was delivered concurrently) or with the words "no shock." In the ambiguity condition, the original "risky" CS+ was shown in place of the ambiguous CS+. After 0.5 s, these signs disappeared and 0.7 s later, a fixation cross was shown during the intertrial period. The intertrial interval was jittering between 4.8 s and 7.8 s resulting in a mean trial onset asynchrony of 12.7 s.

Image acquisition

Images were acquired on a 3 T Allegra head scanner (Siemens Medical Systems) with a head coil for RF transmission and signal reception. Field maps were acquired with a standard manufacturer's double echo gradient echo field map sequence (TE, 10.0 and 12.46 ms; TR, 1020 ms; matrix size, 64 × 64), using 64 slices covering the whole head (voxel size, 3 × 3 × 3 mm).

For functional images, we used BOLD signal-sensitive T_2^*-weighted transverse single-shot gradient-echo echo-planar imaging (EPI; flip angle α, 90°; bandwidth BW, 3551 Hz/pixel; phase-encoding (PE) direction, anterior–posterior; bandwidth in PE direction BWPE, 47.3 Hz/pixel; TE, 30 ms; effective TR, 2600 ms). The manufacturer's standard automatic 3D-shim procedure was performed at the beginning of each experiment. Each volume contained 40 slices of 2 mm thickness (1 mm gap between slices; field of view, 192 × 192 mm^2; matrix size, 64 × 64). BOLD sensitivity losses in the orbitofrontal cortex and the amygdala due to susceptibility artifacts were minimized by applying a *z*-shim gradient moment of −0.4 mT/m · ms, a slice tilt of −30°, and a positive PE gradient polarity (Weiskopf et al., 2006, 2007). In two scanning sessions, 377 and 382 functional whole-brain volumes were acquired. The first 4 volumes, or 10.4 s, of each session were discarded to obtain steady-state longitudinal magnetization. Each session was concluded by 8 volumes, or 20.8 s, without stimuli.

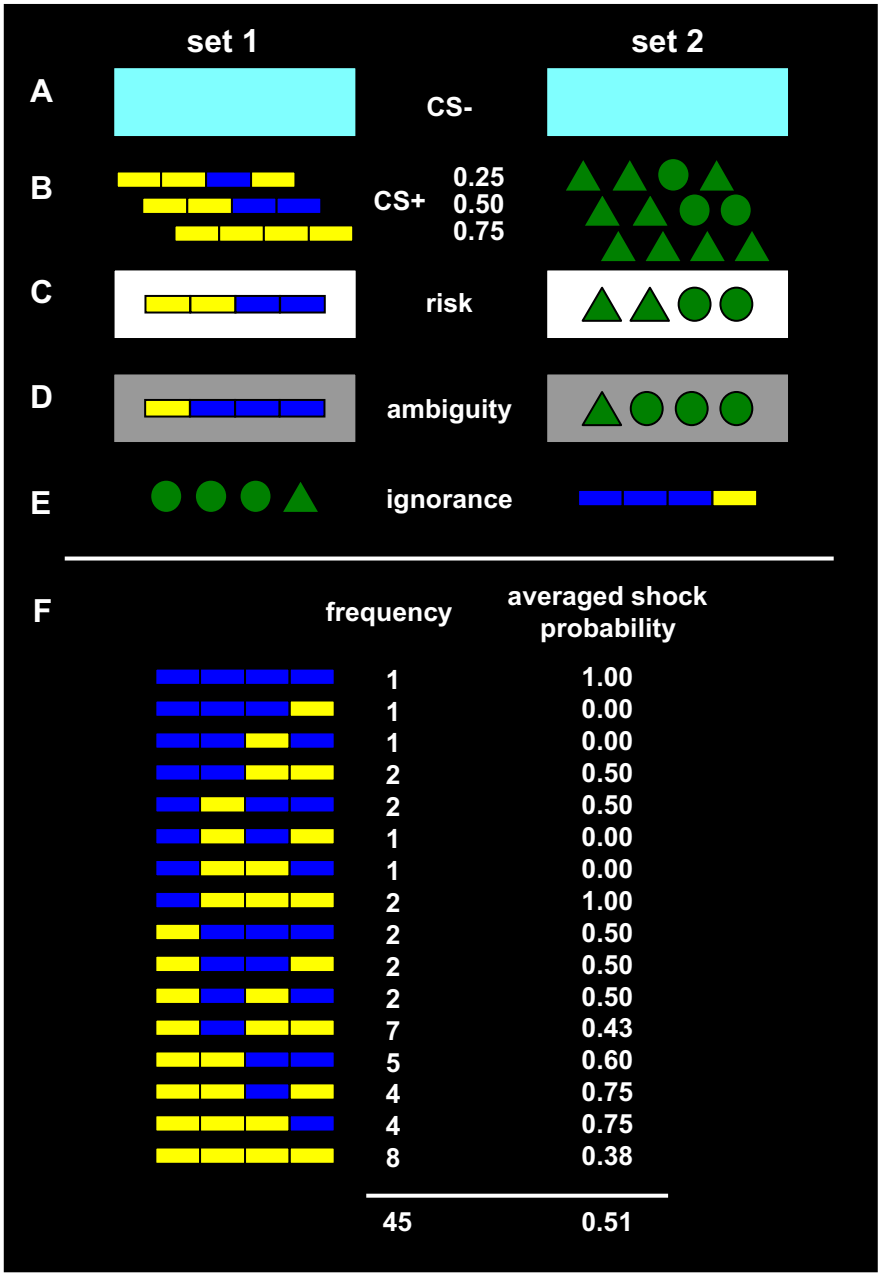

Figure 2. Stimulus set 1 (left) and 2 (right) each of which were used on half of the participants to exclude condition effects due to simple graphical differences. ***A***, CS− that was unchanged throughout the experiment, both in the preceding learning task and at test. ***B***, Three CS+ that were used in the preceding learning task with different CS–UCS contingencies of 0.25, 0.50, and 0.75 as indicated. ***C***, Risk condition used the three original CS+ cues and was signaled by a white frame around the original CS+. ***D***, Example for an ambiguous stimulus, derived from stimulus ***C*** by flipping one of its information bits. The ambiguity condition was signaled by a gray frame around the degraded CS+. ***E***, Example for a novel stimulus, corresponding to stimulus ***D*** by exchanging colors and geometric symbols, and reversing its information bits from left to right. ***F***, All 16 possible ambiguous cues from set 1 (similarly for set 2 with geometric symbols instead of color bars). Each cue was surrounded by a gray frame (omitted in the figure). For each cue, its frequency during the whole experiment is indicated as well as the probability of electric shock after this cue, averaged over the whole experiment. Both frequency and shock probability were determined by the chance that this cue was derived from any of the three underlying risky cues, given a noise rate of 0.2 per information bit.

Whole-brain anatomical scans were acquired using a modified driven equilibrium Fourier transform (MDEFT) sequence with optimized parameters as described previously (Deichmann et al., 2004). One hundred seventy-six sagittal partitions were acquired with an image matrix of 256 × 224 (read × phase) and twofold oversampling in read direction (head/foot direction) to prevent aliasing (isotropic spatial resolution 1 mm; α, 15°; TR/TE/TI, 7.92 ms/2. 4 ms/910 ms; BW, 195 Hz/pixel). Spin tagging in the neck was performed to avoid flow artifacts in the vicinity of

A

	preceding Pavlovian conditioning 80 trials		scanning study 150 trials (2 sessions)		
			risk	ambiguity	ignorance
outcome probability	.75	20 trials	45 trials	45 trials	45 trials
	.50	20 trials			
	.25	20 trials			
	.00	20 trials	15 trials		

B

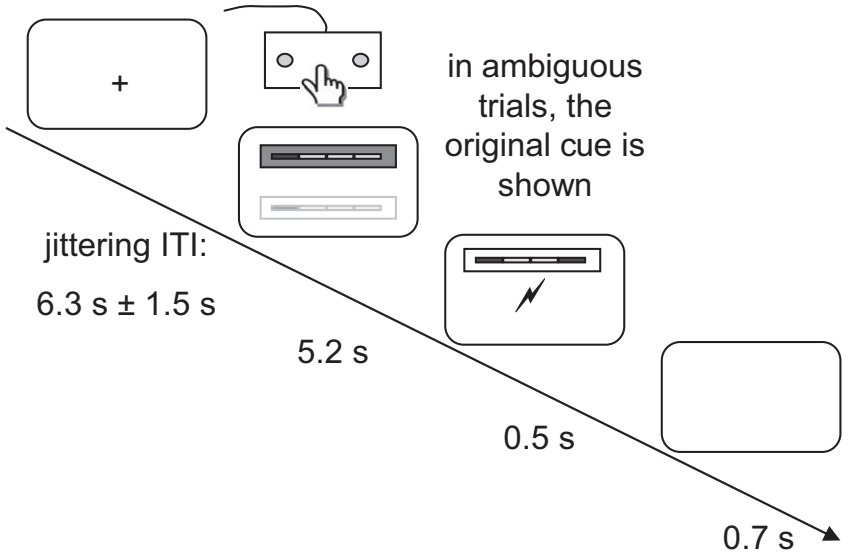

Figure 3. ***A***, Study design. After an initial pavlovian conditioning task with one CS− and three CS+ indicating three different outcome contingencies of 0.25, 0.5, and 0.75, these CS+ were degraded in an ambiguity condition to resemble the original CS+ but allow no accurate prediction of outcomes. This was explained to participants as "noisy reception" and indicated by a gray frame. The original cues were shown in a risk condition as indicated by a white frame. In an ignorance condition, completely novel stimuli served as control. Additionally, the CS− was interleaved and served as internal baseline. ***B***, Intratrial timeline. Each cue was shown for 5.2 s, during which participants had to respond to its position on the screen (above or below the screen center). Then, the outcome was indicated for 0.5 s and delivered. In ambiguous trials, the underlying original CS+ was shown together with the outcome indication. ITI, Intertrial interval.

blood vessels. The flip angle of the tagging pulse was chosen to be 160° to account for B1 losses in the neck. Special RF excitation pulses were used to compensate for B1 inhomogeneities of the transmit coil in superior/inferior and anterior/posterior directions. Images were reconstructed by performing a standard 3D Fourier Transform, followed by modulus calculation. No data filtering was applied in *k*-space or in the image domain.

Image analysis

Images analyzed with statistical parametric mapping (SPM 5; Wellcome Trust Centre for Neuroimaging; www.fil.ion.ucl.ac.uk/spm) on Matlab (version 7.1., MathWorks). EPI images were generated off-line from the complex *k*-space raw data using a generalized reconstruction method based on the measured EPI *k*-space trajectory to minimize ghosting. They were then corrected for geometric distortions caused by susceptibility-induced field inhomogeneities. A combined approach was used which corrects for both static distortions and changes in these distortions due to head motion (Andersson et al., 2001; Hutton et al., 2002). The static distortions were calculated for each subject from a field map that was processed using the FieldMap toolbox as implemented in SPM5. Using these parameters, the EPI images were then realigned and unwarped, a procedure that allows the measured static distortions to be included in the estimation of distortion changes associated with head motion. The motion-corrected images were then coregistered to the individual's anatomical MDEFT image using a 12-parameter affine transformation, and normalized to the Montreal Neurological Institute (MNI) T1 reference brain template (resampled voxel size $2 \times 2 \times 2$ mm). Normalized images were smoothed with an isotropic 8 mm full-width-at-half-maximum Gaussian kernel. The time series in each voxel were high-pass filtered at 1/128 Hz to remove low-frequency confounds. We modeled the presentation of cues for each trial type as a separate boxcar regressor convolved with a canonical hemodynamic response function. In fear conditioning studies, phasic responses to CS+ onset are often observed in the amygdala (see, for example, Büchel et al., 1998; Labar et al., 1998) and occur early rather than late during CS+ presentation (Cheng et al., 2007). To assess such responses, we modeled cue onset with a stick function, thus enhancing sensitivity for early responses to cue onset, and analyzed responses to CS+ > CS− and to the shock probability. In both models, outcome onset and outcome valence (shock or no shock) were included as additional regressors. To account for serial acquisition of different slices in one volume, time derivatives for each regressor were included into the model.

Position of cue (and thus, the type of motor response), response latency, motor speed, and the correctness of response were normalized for each participant, convolved with a hemodynamic response function, and, together with their time derivatives, orthogonalized with respect to each other and included into the model as regressors of no interest. Further regressors of no interest were movement parameters derived from the realignment procedure and correction regressors for variance caused by the cardiac cycle (Glover et al., 2000). Statistical parametric maps were generated from linear contrasts of interest (ambiguity > risk, ambiguity >ignorance) in each participant. A second level random effect analysis (RFX) was then performed using one-sample *t* tests on contrast images obtained in each participant for each comparison of interest (df = 19). To identify areas that show an enhanced re-

Table 1. BOLD responses to contrasts of interest

Brain regions	Brodmann area of local maxima	Hemisphere	Voxel number	Voxel *t* score	Montreal Neurological Institute brain template coordinates of local maxima
Ambiguity > risk					
Posterior inferior frontal gyrus	44, 45	Right	50	4.53	52, 14, 14; 58, 10, 26
	44, 9	Left	147	4.87	−52, 10, 26; −42, 2, 30
Posterior superior parietal lobule	7	Right	44	4.41	34, −50, 50; 30, −58, 44
	7	Left	93	4.97	−26, −54, 46
Middle frontal gyrus	9	Right	15	4.22	40, 10, 30
Fusiform gyrus, inferior temporal gyrus, and parahippocampal gyrus*	19	Right	536	5.97	32, −56, −8; 30, −68, −10; 44, −54, −4
Fusiform gyrus and middle temporal gyrus*	37	Left	188	5.41	−44, −58, 0; −52, −60, 2; −28, −68, −10
Ambiguity > ignorance					
Posterior inferior frontal gyrus and middle frontal gyrus	44, 46, 9	Right	605	5.47	42, 16, 24; 58, 16, 16; 44, 4, 28
Posterior inferior frontal gyrus	46	Right	69	4.82	36, 32, 8; 34, 24, 4
Posterior inferior frontal gyrus and middle frontal gyrus	9	Left	232	5.26	−52, 8, 30; −44, 6, 30; −48, 6, 38
Posterior superior and inferior parietal lobule	7	Right	86	4.48	30, −58, 44; 30, −64 , 50
Occipital cortex*	18, 37, 17	Bilateral	4229	8.31	−30, −82, −8; 32, −46, −14; 10, −88, 6
Middle temporal gyrus and precuneus*	19	Left	173	5.27	−34, −82, 20; −28, −76, 38
Conjunction: (ambiguity > risk) and (ambiguity > ignorance)					
Posterior inferior frontal gyrus	9	Right	10	4.0	54, 14, 14
Middle frontal gyrus	44	Right	26	4.17	44, 12, 30
Posterior inferior frontal gyrus	9	Left	69	4.26	−50, 8, 26
Posterior superior parietal lobule	7	Right	3	3.68	30, −60, 44
Fusiform gyrus and parahippocampal gyrus*	19, 37	Right	566	4.77	28, −70, −14; 38, −52, −14; 30, −56, −8
Fusiform gyrus and lingual gyrus*	18, 19	Left	344	5.29	−28, −68, −10; −20, −74, −12; −26, −80, −8

All clusters are reported at a voxel-level significance threshold of $p < 0.001$, small-volume corrected with $p < 0.05$ for familywise error (FWE) in regions of interest for a 15 mm sphere around peak coordinates as reported by Huettel et al. (2006), and cluster-level corrected with $p < 0.05$ for FWE outside regions of interest (marked *).

sponse to ambiguity compared with both other conditions, a conservative conjunction analysis was performed on the second level, testing against conjunction null (Friston et al., 2005; Nichols et al., 2005). We report clusters with a voxel-level threshold of $p < 0.001$ (uncorrected). In regions of interest for which we had prior hypotheses (posterior inferior frontal gyrus/sulcus, anterior insula, posterior parietal cortex, orbitofrontal and dorsomedial prefrontal cortex, and amygdala), results were small-volume corrected for familywise error within a sphere of 15 mm diameter around peak coordinates as reported by Huettel et al. (2006) and Hsu et al. (2005), and reported at a voxel-level threshold of $p < 0.05$. For the conjunction analysis, small-volume correction was performed on peak coordinates from main contrasts. BOLD responses outside of regions of interest are reported at a cluster-level threshold of $p < 0.05$, whole-brain corrected for familywise error.

Behavioral data analysis

The effect of the condition factor on reaction time measures and task performance was analyzed in a one-way factorial design, using GLM procedures in SPSS 12.0.

Results

Pavlovian conditioning

During pavlovian conditioning, anticipatory skin conductance responses (conditioned reactions, CR) were greater for the CS+ than for the CS− ($F_{(1,12)} = 22.9$; $p < 0.001$). Predicted outcome was significantly correlated with CR ($t_{(13)} = 2.4$; $p < 0.05$), showing that participants learned the CS–UCS contingencies. After conditioning, we tested for typical brain responses associated with conditioned stimuli. By modeling phasic responses to predictive cue onset we observed enhanced activity in left amygdala for the contrast of CS+ (i.e., risky cues) compared with CS−, surviving small-volume correction with a sphere of 15 mm diameter around peak coordinates reported previously for phasic amygdala responses in fear conditioning (Morris and Dolan, 2004). Across the three CS+, activity in the ventral striatum showed a linear increase with increasing probability of negative outcome, surviving small-volume correction with a sphere of 15 mm diameter around peak coordinates reported for representation of outcome probability (Tobler et al., 2007) (additional information can be found in supplemental Table 1, available at www.jneurosci.org as supplemental material).

Behavioral responses to the concurrent task

During the critical phase of the experiment, participants were tasked to respond to the position of the cue, to provide a broad measure for attention. Thus, we were able to test whether our experimental manipulation influenced cognitive processes related to a concurrent task. There was no effect of the condition factor on mean and variance of overall reaction times or response latency, or on task performance ($p > 0.30$ for all ANOVAs).

BOLD responses to contrasts of interest

Our critical contrasts of interest related to the postlearning period and involved evoked responses to presentation of ambiguous and risky, and ambiguous and ignorance cues, respectively. Enhanced differential responses to ambiguous compared with risky stimuli were found bilaterally in posterior inferior frontal gyrus (pIFG), extending into middle frontal gyrus (MFG), and bilaterally in the posterior superior parietal lobule (pPAR) in Brodmann area 7 (Table 1, Fig. 4*A*,*B*). All of these clusters survived small-volume correction around peak coordinates as reported by Huettel et al. (2006). Additional clusters that survived whole-brain correction were found in occipitotemporal cortex including higher visual areas. We did not observe any activation that was greater for risky than for ambiguity cues.

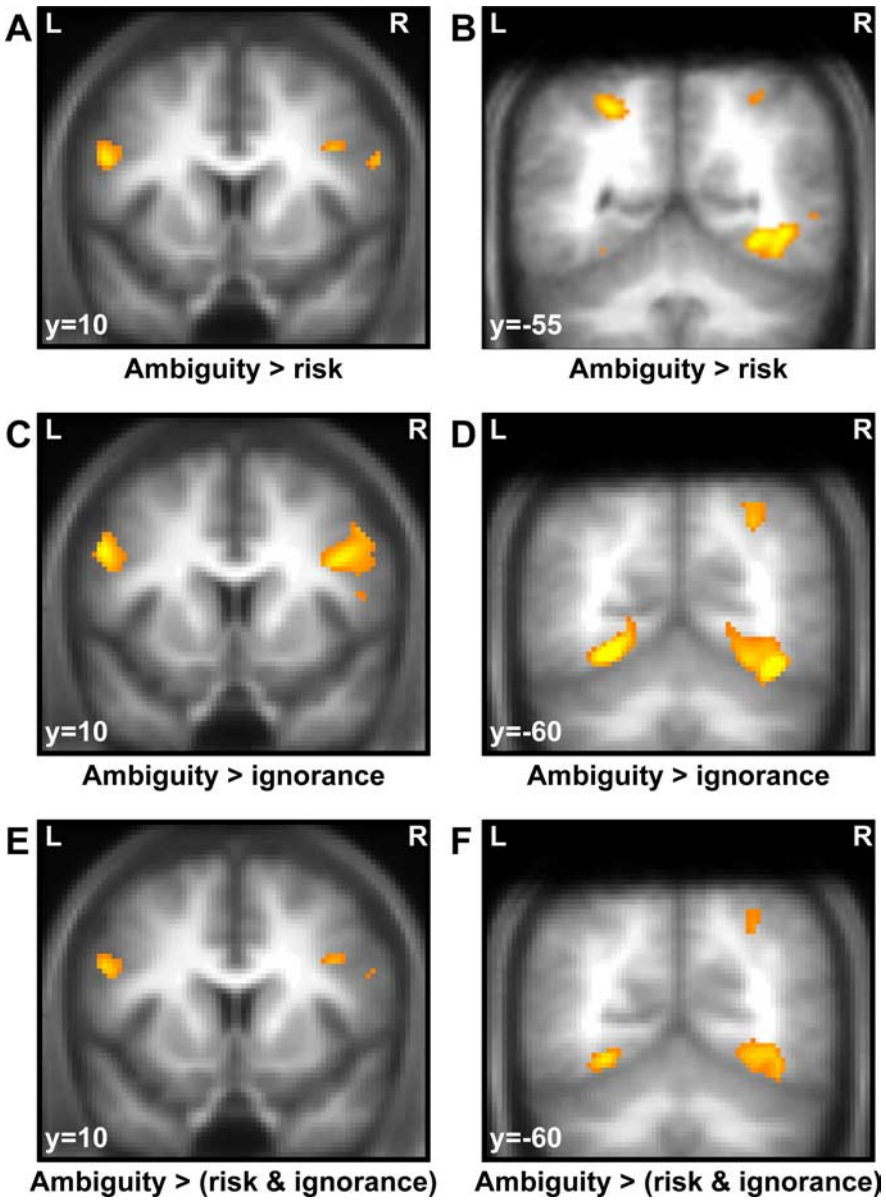

Figure 4. BOLD responses to ambiguous cues, compared with risky or ignorance cues. Clusters are overlaid on a mean T1-weighted image from all participants, and displayed at a voxel-level threshold of $p < 0.001$ (uncorrected) and small-volume correction with regard to peak coordinates of previous studies as indicated in the methods section. ***A***, Bilateral pIFG responses to ambiguous compared with risky cues. ***B***, Bilateral pPAR and occipital responses to ambiguous compared with risky cues. ***C***, Bilateral pIFG responses to ambiguous compared with ignorance cues. ***D***, Right pPAR and bilateral occipital responses to ambiguous compared with ignorance cues. ***E***, Bilateral pIFG responses to ambiguous compared with both risky and ignorance cues (conjunction analysis, testing against conjunction null). ***F***, Right pPAR and bilateral occipital responses to ambiguous compared with both risky and ignorance cues (conjunction analysis, testing against conjunction null).

Our second contrast of interest involving ambiguous compared with ignorance stimuli revealed a set of clusters similar to the above contrast. Specifically, we observed pIFG clusters extending into middle frontal gyrus (MFG) on the right (Fig. 4*C*,*D*). The contrast also showed enhanced posterior parietal responses in the right hemisphere. All of these clusters survived small-volume correction around peak coordinates as reported by Huettel et al. (2006). Additional clusters that survived whole-brain correction were found in occipitotemporal regions. We did not observe activations that were stronger in response to ignorance than to ambiguity cues.

To identify brain areas that showed a greater response to ambiguous than to both risky and ignorance cues, we performed a conjunction analysis. This analysis revealed enhanced responses in bilateral pIFG, extending into right MFG. A small cluster in right pPAR also showed conjoint responses across both contrasts (Figs. 4*E*,*F*, 5). All of these clusters survived small-volume correction around peak coordinates from individual contrasts. Additionally, occipitotemporal areas, including visual areas, responded to ambiguous cues and survived whole-brain correction.

In an exploratory analysis, ignorance and risk were contrasted. No activations were observed that were significantly greater to ignorance than to risk cues. Cerebral responses in the primary visual cortex were greater for risk than for ignorance cues and are summarized in supplemental Table 2 (available at www.jneurosci.org as supplemental material).

Discussion

The present study examined neural responses to perception of ambiguity in the absence of choice. We show that within posterior inferior frontal gyrus (pIFG) and posterior parietal cortex (pPAR), two brain regions previously reported to encode decision making about ambiguous outcomes (Huettel et al., 2006) respond to the perception of ambiguity in the absence of decision making. As our paradigm involved negative outcomes, namely painful electric shocks, it appears brain regions previously associated with ambiguity of reward prediction respond also to ambiguity in aversive predictions. Critically, these responses occur only when a lack of information in outcome predictions could potentially be known. That is, neural responses evoked by ambiguity are not correlated with the distribution width of the outcome prediction, which is highest under complete ignorance, but rather with the fact that information was hidden from the observer.

Economic ambiguity as a contextual cue

The lateral prefrontal cortex (LPFC) is implicated in component processes related to behavioral planning (Lee et al., 2007; Sakagami and Watanabe, 2007; Tanji et al., 2007). Most notably for the present study, where no actual behavior was required in response to the cues, it was suggested that the LPFC is involved in maintaining a state representation in a given environment (Lee et al., 2007). The LPFC area has also been parsed into functionally specific subregions on a dorsal/ventral (Tanji and Hoshi, 2008) or on an anterior/posterior axis (Koechlin and Summerfield, 2007). In the present study, LPFC activation was observed in a posterior dorsal area, the pIFG. It has been suggested that the ventral LPFC is more involved in processing specific, object-related information,

while the dorsal prefrontal cortex is involved in more general functions of monitoring strategic behavior (Tanji and Hoshi, 2008). A framework for a hierarchical anterior/posterior distribution of functions, the cascade model (Koechlin and Summerfield, 2007), proposes that simple stimulus–response relationships are controlled by premotor regions alone, while more contextual cues draw on the posterior prefrontal cortex, with conflicting information drawing on even more anterior regions. Within these two accounts of LPFC subregions, dorsal pIFG activation noted in the present study, as well as in the study by Huettel et al., might reflect a representation of a contextual cue that requires more than mere sensorimotor control. Although in the experimental task, no behavioral response to the cues was necessary, in an everyday environment, economic ambiguity might provide a strong incentive to search for hidden information during an anticipation period, thus overriding simple sensorimotor processes. This search could be under the control of pIFG, even in the absence of an actual decision. This is in line with a previous study examining a noneconomic context and showing activity in the same areas during outcome prediction when contextual cues implied uncertainty (Huettel et al., 2005). This speculation is also supported by the finding that the pIFG responds to economic situations requiring further information search, for example sudden changes in the reward landscape within a dynamic economic game (Li et al., 2006).

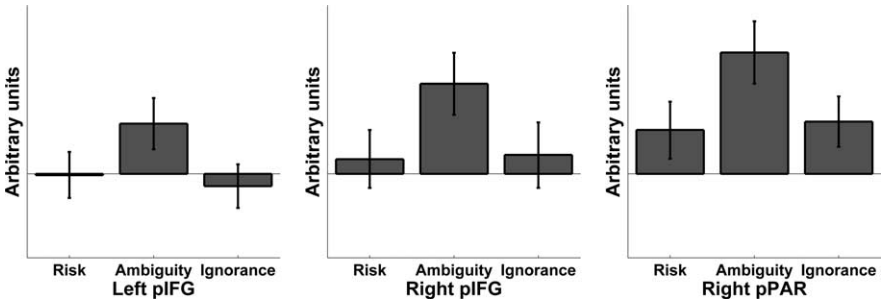

Figure 5. Parameter estimates for the three conditions risk, ambiguity, and ignorance, contrasted with the CS− that served as internal baseline. For each participant, estimates were averaged within the clusters displayed in Figure 4, *E* and *F*. Values are stated in arbitrary units (mean across participants ± SE).

We found a region within pPAR (namely BA 7) activated in response to ambiguity as opposed to risk and ignorance. This area shares connections with the prefrontal cortex (Tanji and Hoshi, 2008) which have been suggested to convey integrated sensory information to executive areas, the strength of which may mediate the effectiveness of executive control (Jung and Haier, 2007). Parietal areas responsible for sensory integration represent a critical decision variable in perceptual decision making (Gold and Shadlen, 2007) and are implicated in valuation of economic choices (see, for example, Platt and Glimcher, 1999; Dorris and Glimcher, 2004; Glimcher et al., 2005). The responses we observed in this region can be construed as reflecting value calculations, and these calculations are necessarily more complex for ambiguous than for risky or ignorance trials due to the second-order probability distribution of ambiguous outcomes. However, since experimental cues differed not only in the information they conveyed but also in color and shape, pPAR responses could conceivably reflect these sensory differences. We think this is unlikely given that differences in these sensory attributes would be expected to be reflected in differential responses in earlier stages of processing, such as visual areas in the occipital cortex.

Finally, a competing explanation for different responses between conditions relates to general attentional differences as, for example, between risk and ambiguity. However, our behavioral data indicate no such difference with respect to reaction time measures and task performance. For additional control, we also covaried reaction times and task performance out of the BOLD signal. Finally, we note there is no easy formalization of attention and in so far as risk and ambiguity embody greater or lesser requirements for information search then it can be argued that each of these processes necessarily entail different levels of attention.

Economic ambiguity and uncertainty of outcome

It has been argued that the critical feature of economic ambiguity is a lack of information (Ellsberg, 1961). In economic studies, this is often operationalized as gambles including a second-order distribution of outcome probabilities (Becker and Brownson, 1964; Larson, 1980; Curley et al., 1986; Pulford and Colman, 2008), which implies a probabilistic prediction of outcome probabilities. This key concept of lack of information about outcome probabilities has been translated as uncertainty of outcomes, or the distribution width of outcome predictions (Yates and Zukowski, 1976). In our experiment, any measure of distribution width of possible outcomes is highest for ignorance and lowest for the risk condition. Since in many experiments on economic ambiguity, the second-order outcome is hidden from the observer, an alternative view involves reformulation of economic ambiguity as "not knowing relevant information that could be known" (Camerer, 1995; p. 645). This quantity is highest in the ambiguity condition in our study.

We failed to identify any brain region responding to uncertainty of outcomes that showed greater responses for ignorance over ambiguity and at the same time for ambiguity over risk. Indeed, virtually all neural responses to ambiguity compared with risk were also evident when ambiguity was compared with ignorance. Therefore, the critical aspect of ambiguity in our experiment, in terms of observable neural activity, was not uncertainty in itself but the fact that the missing information was hidden to the observer and could potentially be revealed. This fits an interpretation of ambiguity as a contextual cue necessitating further search for information before the outcome occurs, i.e., during the anticipation period. In contrast, under complete ignorance of outcome distributions, an optimal strategy might involve sampling from outcomes rather than looking for information in the environment. This is reflected in phenomena such as novelty seeking (Wittmann et al., 2008), as opposed to ambiguity aversion. The potential to gain knowledge of hidden outcome information is therefore a critical factor for brain responses observed here.

One could argue that in the study by Huettel et al. (2006) that showed similar brain responses as our study, ambiguous gambles in fact involved a uniform outcome probability distribution, and that this translates as complete ignorance. The intratrial design of this experiment however strongly emphasized the fact that probabilities were merely hidden rather than unknown, since they were revealed after a decision had been made. This is very similar to our own study where underlying risky cues were shown during the outcome phase of ambiguous trials, thus emphasizing the fact that there was information present that could potentially be re-

vealed, and therefore makes our results on the effect of ambiguity over ignorance compatible with those of Huettel et al. (2006).

An alternative explanation for these findings relates to the computational demand which is also highest in the ambiguity condition compared with both other condition. Both explanations however indicate that uncertainty of outcomes is not the factor modulating cerebral responses in the present study. Whether it is also critical for actual economic decisions under ambiguity cannot be answered within our paradigm.

Ambiguity and the amygdala

In contrast to the present experiment, a previous fMRI study has suggested that the amygdala and dorsomedial prefrontal and orbitofrontal cortex underlie decision making under ambiguity (Hsu et al., 2005). This is consistent with a framework of the amygdala as a detector of ambiguity (Whalen, 1998) elaborated to explain why the amygdala is more activated in response to fearful (that supposedly do not clearly indicate whether a threat is present) than to angry faces (Whalen et al., 2001), and why amygdala responses during fear conditioning quickly habituate [supposedly because they reflect uncertainty about CS–UCS contingencies (Büchel et al., 1998)]. Although it is obvious that the amygdala responds to some kinds of uncertainty [e.g., temporal unpredictability (Herry et al., 2007)], different forms of uncertainty have not been formally compared with regard to such responses. The kind of outcome uncertainty described in the aforementioned work is likely to be different from the economic definition applied in the present study (e.g., the lack of knowledge about CS–UCS contingencies in fear conditioning paradigms corresponds to the ignorance and not the ambiguity condition in the present study). The study by Hsu et al. (2005), although concerned with an economic definition of ambiguity, in fact collapsed different kinds of "ambiguous" situations for analysis of fMRI data, that is, monetary gambles following a strict economic definition, but also quizzes, and uninformed gambles against an informed opponent. Together, the data indicate that there is no entirely convincing empirical evidence that the amygdala responds to ambiguity as defined in a strict economic sense, an inference upheld by our present findings, although such a role of the amygdala cannot be discounted entirely (Seymour and Dolan, 2008).

Individual attitudes to risk and ambiguity

The approach taken in the present paradigm entailed dispensing with any active decisions to study the brain response to perception of stimuli per se. This makes it difficult to directly infer participants' attitudes toward these cues as in terms of formalized neuroeconomic models that incorporate individual risk and ambiguity preferences. Previous imaging studies have shown that neural responses to risky and ambiguous situations might depend on such individual attitudes (Hsu et al., 2005; Huettel et al., 2006). The present study however was not designed to test such relations although we acknowledge their likely importance.

Conclusions

Ambiguity is an important aspect of uncertainty in decision making. Here, we draw on the definition of ambiguity as a lack of information that could potentially be known and operationalized it as a probabilistic prediction of outcomes in a pavlovian conditioning paradigm. In the absence of any decisions, we show that a network comprising the pIFG and pPAR responds to the perception of ambiguity as opposed to risk (point estimate of outcome probabilities) or ignorance (uniform distribution of outcome probabilities). This corresponds to a network previously been implicated in decisions involving ambiguity. We conclude that the critical factor for these responses to ambiguity is anticipation of an outcome when information about outcome probabilities is hidden, but potentially knowable. pIFG responses might subserve contextual analysis when search of hidden information is both necessary and meaningful before the occurrence of an outcome.

References

Andersson JL, Hutton C, Ashburner J, Turner R, Friston K (2001) Modeling geometric deformations in EPI time series. Neuroimage 13:903–919.

Becker SW, Brownson FO (1964) What price ambiguity? Or the role of ambiguity in decision making. J Polit Econ 72:62–73.

Bernoulli D (1738) Specimen theoriae novae de mensura sortis. Commentarii Academiae Scientiarum Imperialis Petropolitanae 5:175–192.

Büchel C, Morris J, Dolan RJ, Friston KJ (1998) Brain systems mediating aversive conditioning: an event-related fMRI study. Neuron 20:947–957.

Camerer C (1995) Individual decision making. In: Handbook of experimental economics (Kagel JH, Roth AE, eds), pp 587–704. Princeton: Princeton UP.

Cheng DT, Richards J, Helmstetter FJ (2007) Activity in the human amygdala corresponds to early, rather than late period autonomic responses to a signal for shock. Learn Mem 14:485–490.

Curley SP, Yates F, Abrams RA (1986) Psychological sources of ambiguity avoidance. Organ Behav Hum Decis Process 38:230–256.

Dayan P, Balleine BW (2002) Reward, motivation, and reinforcement learning. Neuron 36:285–298.

Deichmann R, Schwarzbauer C, Turner R (2004) Optimisation of the 3D MDEFT sequence for anatomical brain imaging: technical implications at 1.5 and 3 T. Neuroimage 21:757–767.

Dorris MC, Glimcher PW (2004) Activity in posterior parietal cortex is correlated with the relative subjective desirability of action. Neuron 44:365–378.

Ellsberg D (1961) Risk, ambiguity, and the Savage axioms. Q J Econ 75:643–669.

Friston KJ, Penny WD, Glaser DE (2005) Conjunction revisited. Neuroimage 25:661–667.

Glimcher PW, Dorris MC, Bayer HM (2005) Physiological utility theory and the neuroeconomics of choice. Games Econ Behav 52:213–256.

Glover GH, Li TQ, Ress D (2000) Image-based method for retrospective correction of physiological motion effects in fMRI: RETROICOR. Magn Reson Med 44:162–167.

Gold JI, Shadlen MN (2007) The neural basis of decision making. Annu Rev Neurosci 30:535–574.

Herry C, Bach DR, Esposito F, Di Salle F, Perrig WJ, Scheffler K, Lüthi A, Seifritz E (2007) Processing of temporal unpredictability in human and animal amygdala. J Neurosci 27:5958–5966.

Hsu M, Bhatt M, Adolphs R, Tranel D, Camerer CF (2005) Neural systems responding to degrees of uncertainty in human decision-making. Science 310:1680–1683.

Huettel SA, Song AW, McCarthy G (2005) Decisions under uncertainty: probabilistic context influences activation of prefrontal and parietal cortices. J Neurosci 25:3304–3311.

Huettel SA, Stowe CJ, Gordon EM, Warner BT, Platt ML (2006) Neural signatures of economic preferences for risk and ambiguity. Neuron 49:765–775.

Hutton C, Bork A, Josephs O, Deichmann R, Ashburner J, Turner R (2002) Image distortion correction in fMRI: A quantitative evaluation. Neuroimage 16:217–240.

Jung RE, Haier RJ (2007) The Parieto-Frontal Integration Theory (P-FIT) of intelligence: converging neuroimaging evidence. Behav Brain Sci 30: 135–154; discussion 154–187.

Koechlin E, Summerfield C (2007) An information theoretical approach to prefrontal executive function. Trends Cogn Sci 11:229–235.

LaBar KS, Gatenby JC, Gore JC, LeDoux JE, Phelps EA (1998) Human amygdala activation during conditioned fear acquisition and extinction: a mixed-trial fMRI study. Neuron 20:937–945.

Larson JR (1980) Exploring the external validity of a subjectively weighted utility model of decision making. Organ Behav Hum Perform 26:293–304.

Lee D, Rushworth MF, Walton ME, Watanabe M, Sakagami M (2007) Functional specialization of the primate frontal cortex during decision making. J Neurosci 27:8170–8173.

Li J, McClure SM, King-Casas B, Montague PR (2006) Policy adjustment in a dynamic economic game. PLoS ONE 1:e103.

Morris JS, Dolan RJ (2004) Dissociable amygdala and orbitofrontal responses during reversal fear conditioning. Neuroimage 22:372–380.

Nichols T, Brett M, Andersson J, Wager T, Poline JB (2005) Valid conjunction inference with the minimum statistic. Neuroimage 25:653–660.

Oldfield RC (1971) The assessment and analysis of handedness: the Edinburgh inventory. Neuropsychologia 9:97–113.

Platt ML, Glimcher PW (1999) Neural correlates of decision variables in parietal cortex. Nature 400:233–238.

Pulford BD, Colman AM (2008) Size doesn't really matter. Ambiguity aversion in Ellsberg urns with few balls. Exp Psychol 55:31–37.

Rangel A, Camerer C, Montague PR (2008) A framework for studying the neurobiology of value-based decision making. Nat Rev Neurosci 9:545–556.

Rescorla RA, Wagner AR (1972) A theory of pavlovian conditioning: Variations in the effectiveness of reinforcement and nonreinforcement. In: Classical conditioning II: current research and theory (Black AH, Prokasy WF, eds), New York: Appleton-Century-Crofts.

Sakagami M, Watanabe M (2007) Integration of cognitive and motivational information in the primate lateral prefrontal cortex. Ann N Y Acad Sci 1104:89–107.

Seymour B, Dolan R (2008) Emotion, decision making, and the amygdala. Neuron 58:662–671.

Slovic P, Tversky A (1974) Who accepts Savage's axiom? Behav Sci 19:368–373.

Tanji J, Hoshi E (2008) Role of the lateral prefrontal cortex in executive behavioral control. Physiol Rev 88:37–57.

Tanji J, Shima K, Mushiake H (2007) Concept-based behavioral planning and the lateral prefrontal cortex. Trends Cogn Sci 11:528–534.

Tobler PN, O'Doherty JP, Dolan RJ, Schultz W (2007) Reward value coding distinct from risk attitude-related uncertainty coding in human reward systems. J Neurophysiol 97:1621–1632.

von Neumann J, Morgenstern O (1944) Theory of games and economic behavior. Princeton: Princeton UP.

Weiskopf N, Hutton C, Josephs O, Deichmann R (2006) Optimal EPI parameters for reduction of susceptibility-induced BOLD sensitivity losses: a whole-brain analysis at 3 T and 1.5 T. Neuroimage 33:493–504.

Weiskopf N, Hutton C, Josephs O, Turner R, Deichmann R (2007) Optimized EPI for fMRI studies of the orbitofrontal cortex: compensation of susceptibility-induced gradients in the readout direction. MAGMA 20:39–49.

Whalen PJ (1998) Fear, vigilance and ambiguity: initial neuroimaging studies of the human amygdala. Curr Dir Psychol Sci 7:177–188.

Whalen PJ, Shin LM, McInerney SC, Fischer H, Wright CI, Rauch SL (2001) A functional MRI study of human amygdala responses to facial expressions of fear versus anger. Emotion 1:70–83.

Wittmann BC, Daw ND, Seymour B, Dolan RJ (2008) Striatal activity underlies novelty-based choice in humans. Neuron 58:967–973.

Yates JF, Zukowski LG (1976) Characterization of ambiguity in decision-making. Behav Sci 21:19–25.